Burstlike first-order transformation studied by semi-adiabatic relaxation calorimetry

Vincent Hardy, Radia Hamane, Xavier Larose, Michel Risser, François Guillou

Burstlike first-order transformation studied by semi-adiabatic relaxation calorimetry

V Hardy[1,a)], R. Hamane[1], X. Larose[1], M. Risser[2] and F. Guillou[3]

AFFILIATIONS

1- Normandie University, ENSICAEN, UNICAEN, CNRS, CRISMAT, 14000 Caen, France
2- UbiBlue, 23 Boulevard de l'Orangerie, 67000 Strasbourg, France
3- Inner Mongolia Key Laboratory for Physics and Chemistry of Functional Materials, Inner Mongolia Normal University, 81 Zhaowuda Road, Hohhot 010022, Inner Mongolia, People's Republic of China

a) Author to whom correspondance should be addressed: vincent.hardy@ensicaen.fr

ABSTRACT

This paper reports on a mode of analysis of semi-adiabatic relaxation data allowing to account for exotic phenomena sometimes observed in first-order transitions. The principal interest is to get a detailed characterization of the latent heat while using the same experimental configuration as that employed for accurate heat capacity measurements outside the transition. Special attention is paid to the recalescence/antirecalescence effects as well as to the existence of spikes in the time-dependent exchange of latent heat. The present approach —based on the notion of "power of latent heat"— is shown to be consistent with differential scanning calorimetry, magnetization measurements and the usual analysis in terms of heat capacity. The study is carried out on a $LaFe_{10.77}Si_{1.23}Co_{0.28}$ compound which belongs to one of the most promising families of giant magnetocaloric materials.

I. INTRODUCTION

First-order transitions (FOT) are characterized by the presence of a latent heat and a regime in which two phases coexist. These features are known to complicate the experimental characterizations of this type of transition, while they are also prone to trigger various striking phenomena. One among the best known examples is that of recalescence which has been observed since a long time at the solidification of some metallic compounds [1-2]. Basically, this phenomenon corresponds to a transient increase of temperature as the material crosses the transition upon cooling, and its origin relies on a sudden release of latent heat. This phenomenon can also take place at magnetic transitions, as exemplified by the case of iron reported at the end of the nineteenth century [3]. More recently, related effects have been studied in several magnetic materials for which the symmetrical phenomenon of temperature decrease when crossing the transition upon warming (so-called antirecalescence) was also observed [4-5]. The origin of these phenomena, in particular their connection with the presence of structural defects within the material, was intensively debated. While Gschneidner

et al.[4] claimed the requirement of a high purity in the case of Er, Bag *et al.* [5] rather pointed to the key role of an inhomogeneous microstructure in their study of (Hf,Ta)Fe_2. Along the paper, we will adopt the denomination of "*reversed trend*" in the thermal response to refer to both the recalescence and antirecalescence phenomena.

First-order transitions are also known to potentially exhibit burst-like transitions, i.e. a regime where the transformation from one phase to the other proceeds via a succession of steps. There is an obvious link with the previous phenomena of recalescence/antirecalescence in that the sudden heat flux associated to a burst can be hardly absorbed by the thermalisation of the experimental set-up. Calorimetric characterization of burstlike transitions is tricky. Partly due to the intense activity on the magnetocaloric materials in the recent years, a lot of advances have emerged on this issue. A crucial step was reached by the development of the Differential Scanning Calorimetry (DSC) equipments based on Peltier cells which are able to directly quantify the exchange of heat flux between the sample and the thermal sink [6-9]. This approach has allowed to demonstrate that the heat exchange at the FOT of some materials can take the form of a succession of individual peaks distributed over a certain interval of time [10-11]. This peculiar manifestation give rise to "spiky patterns", a denomination we will adopt along the present paper.

The most common method for specific heat measurements nowadays is the semi-adiabatic relaxation technique,[12] which is at the basis of widespread commercial devices, e.g. [13]. Coupled with an analysis involving two relaxation times,[14] this method is very well suited for second-order transitions, while it is in principle reliable only outside the transition regime for FOT's. However, special modes of measurements/analysis have been proposed to overcome the difficulties associated to the FOT, allowing for instance the characterization of a sharp peak-like transition or the broad transitional regime of a martensitic-like transition [15-18].

It turns out that the combination of "reversed trends" and "spiky patterns" brings with it a new challenge, which has not been addressed so far to the best of our knowledge. This is the aim of the present paper to show that a specific analysis of relaxation data allows to identify the above-mentioned phenomena. The paper is organized as follows: in a first part, we present the model allowing to derive instantaneous heat flux exchanges versus time; in a second part, the model is applied to measurements on a LaFeSiCo alloy; the third part is intended to support the reliability of the analysis by comparing the results to DSC data, and by showing the consistency with the overall latent heat derived from the Clausius-Clapeyron (CC)

equation. In a last part, the results of the model are also compared to the standard analysis in terms of heat capacity.

II. EXPERIMENTAL DETAILS

This study is carried out on thin platelet-shaped samples (~ 2.2×2.2×0.4 mm^3) of a LaFeSiCo alloys provided by Vacuumschmelze GmbH and CoKG. The compositional analysis carried out by energy-dispersive X-ray spectroscopy (Bruker Xflash) within a scanning electron microscope (JEOL 7200 LV) leads to the approximate formula $LaFe_{10.77}Si_{1.23}Co_{0.28}$. This compound undergoes a Curie transition around 207 K (with a thermal hysteresis of the order of 1 K), accompanied by an isotropic change of volume of about 1% (larger in the ferromagnetic state) [19-20].

The heat capacity measurements were carried out with the semi-adiabatic relaxation option of a Physical Properties Measurements System (PPMS, Quantum Design) on a 15.3 mg sample. We used the so-called "vertical puck" which is suited to measurements in non-zero magnetic fields (1 T in the present case), for two mains reasons : (i) the magnetic field is within the plane of the sample, which ensures a small demagnetizing effect; (ii) the sample lies in a region of constant field, which avoids a magnetic force to be exerted on the sample [21].

Another sample of the same batch and of the same shape (16.2 mg) was investigated by DSC in zero-field. This experiment was carried in a TA instruments DSC 2500 Tzero technology and using Al crucibles.

Magnetic measurements were carried out in the PPMS by using a third sample of the same batch (and of the same shape with a mass of 15.9 mg). Isothermal magnetization curves were recorded with the field applied within the plane of the sample, as for the heat capacity measurements.

III. RESULTS

Figure 1 shows the thermal response of the platform onto which is pasted the sample when submitted to a large heat pulse, making it to cross the transition both along the warming and cooling branches. Along each transition regime, one observes a "reversed trend" of the measured temperature, exhibiting a negative average $<dT_p/dt>$ upon warming and a positive one upon cooling. Moreover, the enlargement of the FM-to-PM transition displayed in the bottom inset shows some "modulations" on the temperature profile which can be regarded as

the fingerprints of underlying peaks in the flux heat exchange. It is important to emphasize that the reversed trends and spiky patterns are separate features which are not intrinsically linked to each other. As a matter of fact, Pecharsky *et al.* observed reversed trends in pure Dy without any indication of peaks, [22] and we will see later that our material still exhibits some small peaks in a magnetic field of 1 T but without reversed trends. What is common to both features is that a sign of dT_p/dt opposed to the standard ones (either instantaneous values or averaged over the transition "plateau") precludes an analysis in terms of heat capacity.

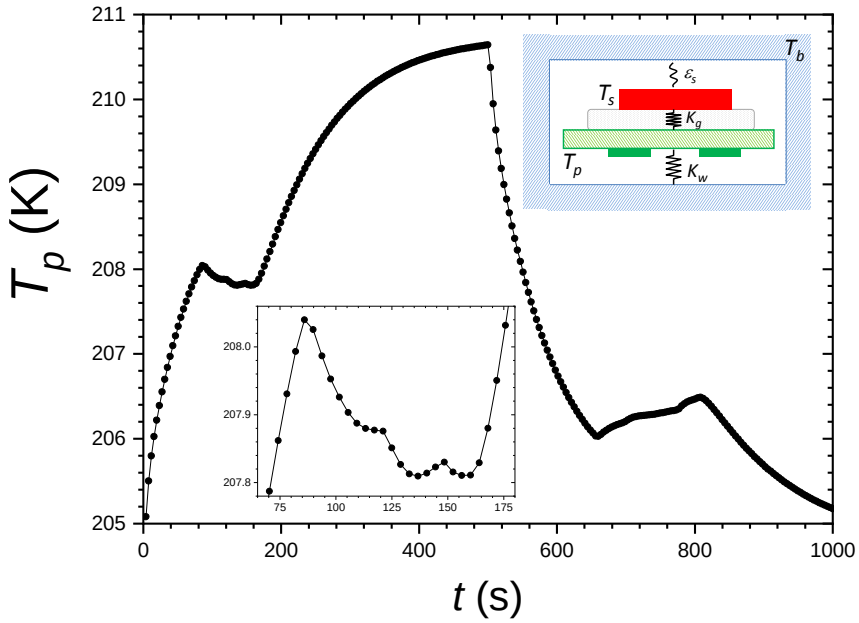

FIG. 1. Example of thermal response to a heat pulse, for the semi-adiabatic relaxation set-up schematically shown in the upper inset. The sample (red) is pasted by a thin layer of Apiezon N (dotted grey) onto a sapphire platform (dashed green), below which are attached a heater and a thermometer (green rectangles). The thermal resistances sample/platform (via the grease) and platform/bath (via the wires) are denoted K_g and K_w, respectively. A radiative link between the sample surface and the cap at the base temperature involves the emissivity ε_s. The temperature T_s, T_p and T_b are those of the sample, platform and bath, respectively. The bottom inset is an enlargement of the transitional regime along the heating branch, which clearly exhibits a "reversed trend" (decrease of the average temperature) and a "spiky pattern" (presence of spikes along the transitional regime).

The thermal equations used to describe the system shown in the top inset of Fig 1 are the following

$$C_s \frac{dT_s}{dt} = -K_g\left[T_s - T_p\right] \quad (1a)$$

$$C_{ad} \frac{dT_p}{dt} = P_{heat} - K_w\left[T_p - T_b\right] + K_g\left[T_s - T_p\right] \quad (1b)$$

C_s and C_{ad} are the heat capacities of the sample and of the assembly (platform+grease), respectively; K_g and K_w are the thermal conductances via the grease and through the wires, respectively; T_s, T_p and T_b are the temperatures of the sample, of the platform and of the "bath" or heat sink (i.e. the puck), respectively; P_{heat} is the heating power applied to the

platform during the first branch of the "pulse" (note that we report here the equations of the model used in the standard analysis of the PPMS data, [13] without inclusion of a radiative term). In the standard analysis, the overall $T_p(t)$ response is fitted by the two-τ model allowing to derive an average value of C_s over the pulse range [14]. The investigation of FOT's requires to shift to a point-by-point analysis of the trace (scanning method), which itself requires a thermalisation good enough to assume in first approximation $T_s \sim T_p$ [15-17]. Most often, it is possible to incorporate the latent heat within a generalized view of the specific heat (i.e., combining latent and sensible heats) generating a high, sharp and symmetrical peak at the transition temperature T_{tr} in a $C_s(T)$ plot. Nevertheless, this approach becomes invalidated in case of reversed trends (as leading to "negative heat capacity") and is even disputable in case of peak-like features along the transition regime [23].

In this case, one must go back to a complete reinterpretation of the thermal response at the transition by focusing on the latent heat exchange, while keeping an approach in terms of power. This dual requirement leads us to use the notion of power of latent heat P_L, a quantity corresponding to the fraction of latent heat L exchanged per unit time ($P_L = dL/dt$) and which is actually very comparable to the heat flux values derived in DSC analysis. When addressing the transitional regime (i.e., the plateau-like ranges along the warming and cooling branches) the quantity $P_L(t)$ comes to replace the term $C_s(dT_s/dt)$ in Eq (1a). In other respects, we account for the use of a large temperature increment along the heat pulses (typically 5 K) by revisiting the leak term via the wires, as well as by introducing a radiative term. Indeed, with such large shifts between the platform and sample temperature (T_p and T_s) with respect to the bath (T_b), there is a temperature gradient along the wires that must be taken into account,[17] and a non-negligeable radiative term can emerge between the sample surface and the metallic cap (at T_b). Accordingly, the Eqs (1) are rewritten as follows:

$$P_L(t) = -K_g\left(T_p(t)\right)\left[T_s(t) - T_p(t)\right] - P_{rad}(T_s(t), T_b) \qquad (2a)$$

$$C_{ad}\left(T_p(t)\right)\frac{dT_p(t)}{dt} = P_{heat}(t) - P_{cond}\left(T_p(t), T_b\right) - K_g\left(T_p(t)\right)\left[T_p(t) - T_s(t)\right] \qquad (2b)$$

Combining Eqs (2a) and (2b), (while approximating T_s by T_p in P_{rad}), one obtains

$$P_L(t) \approx P_{heat}(t) - P_{cond}\left(T_p(t), T_b\right) - P_{rad}\left(T_p(t), T_b\right) - C_{ad}\left(T_p(t)\right)\frac{dT_p(t)}{dt} \qquad (3)$$

The derivations of approximate expressions for P_{rad} and P_{cond} are given in the Appendix. From the background measurement of (platform+grease), one can use linear approximations of $C_{ad}(T)$ and of $K_w(T)$ over the T-range of the pulses: $K_w(T) = A + BT$ and $C_{ad}(T) = C + DT$. Gathering all terms in Eq. (3), one obtains a general expression of the

instantaneous power of latent heat over the transitional regime, derived from the thermal response of the platform:

$$P_L(t) \approx P_{heat}(t) - \left\{ \frac{B[T_p(t)-T_b]}{ln\left[\frac{A+BT_p(t)}{A+BT_b}\right]} + 4S\sigma_T\varepsilon_s T_b^3 \right\} \left[T_p(t) - T_b\right] - \left[C + DT_p(t)\right] \frac{dT_p(t)}{dt}. \qquad (4)$$

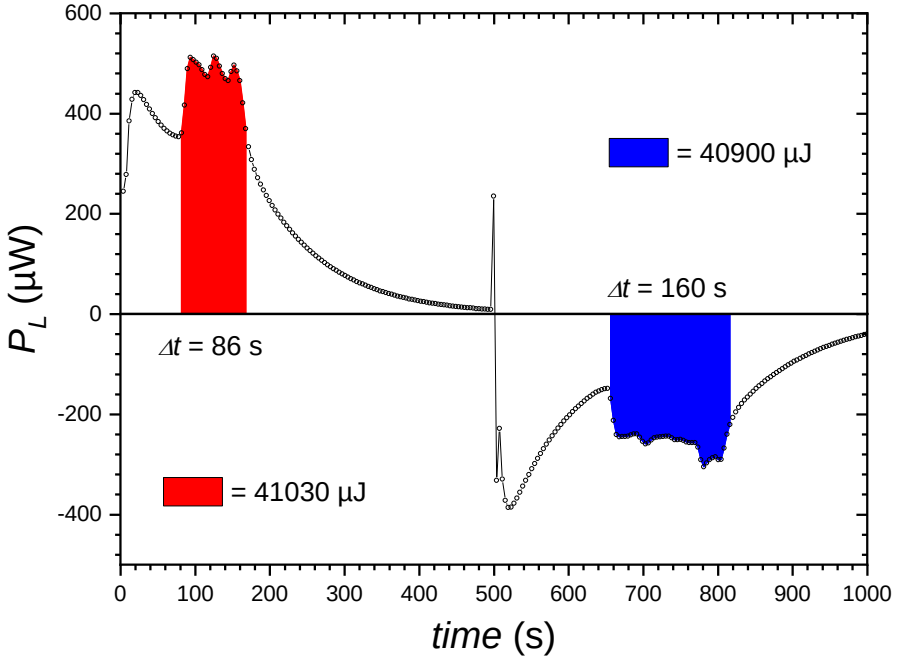

FIG. 2. Analysis of the thermal response of Fig. 1 via Eq. (4), giving the time dependence of the power of latent heat $P_L(t)$. The analysis is shown here over the whole range of data even if it is only meaningful over the transitional ranges, materialized by the colored areas. The durations of these transformations are indicated as Δt. Also reported are the values of the latent heat estimated by the integration of $P_L(t)$ over Δt, both along the warming (red) and cooling (blue) paths.

On the warming branch P_{heat} is the value applied to the platform, while it is zero on the cooling one ; σ_T is the Stefan-Boltzmann constant, S the radiative surface of the sample (~ 5 mm^2), and ε_s its infrared emissivity, for which we will assume the value ~ 0.3 typical of unpolished metallic-like surface. Figure 2 shows the results of Eq. (4) applied to the trace of Fig. (1). Although this analysis is only valid within the plateaus, we present the results over the whole time window to show the difficulty associated to the definition of the boundaries. In practice, we will use the extremum points of the $T_p(t)$ profile. To estimate the overall latent heat, one must integrate $P_L(t)$ over the duration of the transformation. By assuming vertical boundaries in Fig. 2, one obtains close values on the warming and cooling branches, namely 41.03 and 40.90 mJ, respectively.

On both branches, this analysis shows the presence of spikes on $P_L(t)$, and we consider this reflects a burstlike exchange of latent heat. To test the reliability of this view, several

studies have been undertaken: (i) comparison to DSC measurements; (ii) sensitivity of the value $L = \int P_L(t)dt$ to the measuring protocol; (iii) consistency of L with the expected value from the CC equation; and finally (iv) comparison with the standard analysis in terms of *C(T)* when considering data in 1 T (for which the "reversed trends" have vanished).

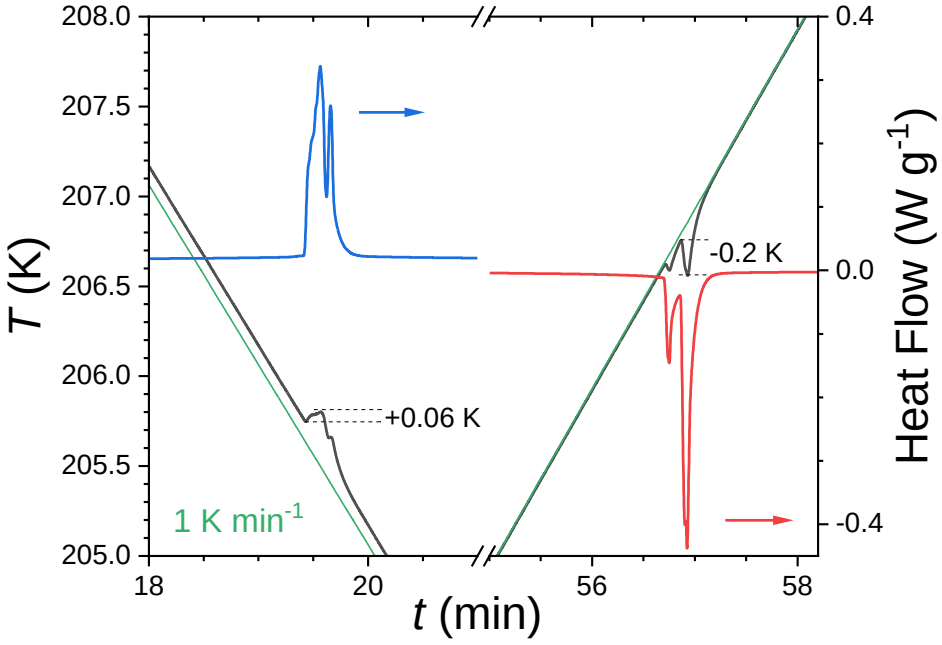

FIG. 3. DSC scans upon cooling and warming across T_{tr} at a rate of 1 K/min. The left axis shows the Tzero temperature of the base (straight, thin lines) and that of the sample (thick lines). The amplitude of the "reversed trends" is evaluated by the dashed lines. The right axis corresponds to the heat flows (obtained with the complete Tzero heat balance equation) which clearly exhibit spikes, both upon warming and cooling.

Figure 3 shows the results of DSC measurements performed at a rate of 1 K/min around T_{tr}. The results are presented both in terms of sample temperature and of heat flow from the sample as a function time. One observes that the response is qualitatively well consistent with that previously obtained from Eq. (4), since one observes reversed trends and spikes of heat flow along the transition. The intensity of the reversed trends is of the same order of magnitude, namely ~ 0.1-0.2 K from DSC versus ~ 0.2-0.4 K in our experiments. The sample mass and temperature rates are very similar in both experiments; the difference most likely originates from the thermal dilution with the crucible in DSC measurements and from the degree of thermal contact sample/base, which is expected to be higher in the DSC setup. We also note that the instantaneous heat flows in DSC have a mean value of ~ 3000 µW which is significantly larger than the one observed in Fig. 2 (while the masses are similar in both cases), but this heat exchange develops over a time interval which is smaller than in our

experiments. Once again, this variation in dynamics might be related to the difference in thermalisation of the two set-ups.

Changing the parameters of the heat pulse (starting temperature, increment and power) modifies substantially the shape of the response. Table I gathers the parameters investigated within a series of heating pulses that were all analyzed with Eq. (4). It turns out that the presence of spikes is always detected in the $P_L(t)$ response, whereas the intensity of the reversed trends can be substantially reduced. In all cases, however, one obtains very consistent values of L.

n	T_b (K)	P_{heat} (µW)	ΔT_{pulse} (K)	L (mJ)
a	205	969	5	41.03
b	206	582	3	41.10
c	203	1340	7	41.43
d	204	962	5	40.85
e	205	773	4	39.55
f	206	582	3	40.11
g	206	777	4	39.42
h	206	971	5	39.53
i	206	1164	6	40.99

TABLE I. Measuring parameters of different heating branches recorded in zero field; T_b is the base temperature (temperature of the "bath"); ΔT_{pulse} is the targeted temperature increment; P_{heat} is the power applied to the heater to generate the pulse. The last column is the value of latent heat derived from integration of $P_L(t)$ over the transitional regime (the mass of the sample is 15.8 mg).

To go further, we have derived an independent estimate of L from the CC equation. Figure 4(a) shows a series of $M(H)$ curves recorded at selected temperatures, from which one can derive the temperature dependence of the transition fields associated to the midpoint of the metamagnetic steps (see the supplementary material); combined with an evaluation of the height of the steps along the transition (ΔM), the CC equation allows to estimate the value of the entropy jump at the transition: $\Delta S_{tr} = -\frac{\Delta M}{(dT_{tr}/dB)}$. The results reported in Fig. 4(b) show a marked decrease in ΔS_{tr} as the field is increased, in accordance with the literature on these LaFeSiCo alloys. Taking into account the experimental uncertainties (mainly on ΔM, see supplementary material) and the relationship $L = T_{tr} \times \Delta S_{tr}$, one obtains that $L(0\mathrm{T}) \sim 2.8 \pm 0.1$ Jg^{-1}. For the sample used in calorimetry (m = 15.8 mg), one thus expects $L(0\mathrm{T}) \sim 44 \pm 2$ mJ, a value slightly larger but well comparable to that derived from $\int P_L(t)dt$ (~ 41 mJ).

To investigate the impact of the magnetic field on the transitional regime, a couple of heat pulses was recorded in our calorimeter with the same value of ΔT_{pulse} and P_{heat}, both in B = 0 T and B = 1 T. Owing to the field dependence of the Curie temperature, the starting temperature was shifted by 4 K for the measurements in field. The results are shown in Fig. 5 by plotting the temperature variation as a function of time. The relative positioning of the two curves is striking: they exhibit similar overall shapes, but the reversed trends present in B = 0 T are totally absent from the curve B = 1 T. In other respects, the enlargement of the transitional regime upon warming (inset) shows the persistence of some modulations on the 1 T trace, even though much smoother than in B = 0 T. This evolution can be ascribed to the reduction of the latent heat in 1 T as reported in Fig. 4(b).

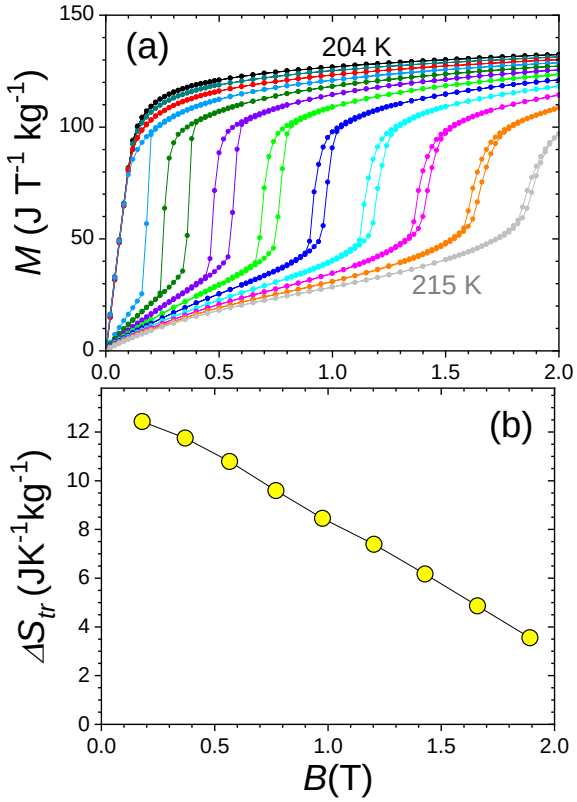

FIG. 4. Isothermal magnetization loops recorded in the range 0-2 T after zero-field cooling. The measurements are carried out with the field applied along the plane of the sample, at temperatures spaced by 1 K between 204 and 215 K. (b) Values of the entropy jump at the transition, derived from the Clausius-Clapeyron equation applied to the ascending branches of the loops in (a).

In practice, the absence of reversed trend allows to handle these 1 T data with the conventional analysis in terms of heat capacity. This approach first consists in turning back to a term $C_s \frac{dT_s}{dt}$ in Eq. 2(a); then, one assumes a coupling sample/platform good enough to consider the set (platform+grease+sample) as a whole at a temperature T_p=T. A point-by-point analysis of the thermal response leads to $C_{tot}(t) \frac{dT(t)}{dt} = P_{heat}(t) - P_{cond}(T(t), T_b) -$

$P_{rad}(T(t), T_b)$, where $C_{tot} = C_s + C_{ad}$. Converting the time dependence into a temperature one, one obtains

$$C_s(T) \approx \left[\frac{P_{heat}(T) - P_{cond}(T,T_b) - P_{rad}(T,T_b)}{(dT/dt)(T)}\right] - C_{ad}(T) \quad (5)$$

In this analysis, the range of time used for the derivative *dT/dt* must be large enough to smooth the "modulations" and ensure average <*dT/dt*> values having the "expected" sign along the transitional regimes. In a last step, a rough correction of the temperature lag between $T = T_p$ and T_s can be applied by using an estimate of K_g (see supplementary material) to generate final results in the form of a $C_s(T=T_s)$ curve. Following this approach with the 1 T data of Fig. 5, one obtains the $C_s(T)$ shown in Fig. 6(a) (transition upon warming). Note that this curve is limited to the *T*-range highlighted by the blue line in Fig. 5, since this analysis is known to generate increased uncertainties at the beginning and end of the pulse [15-17].

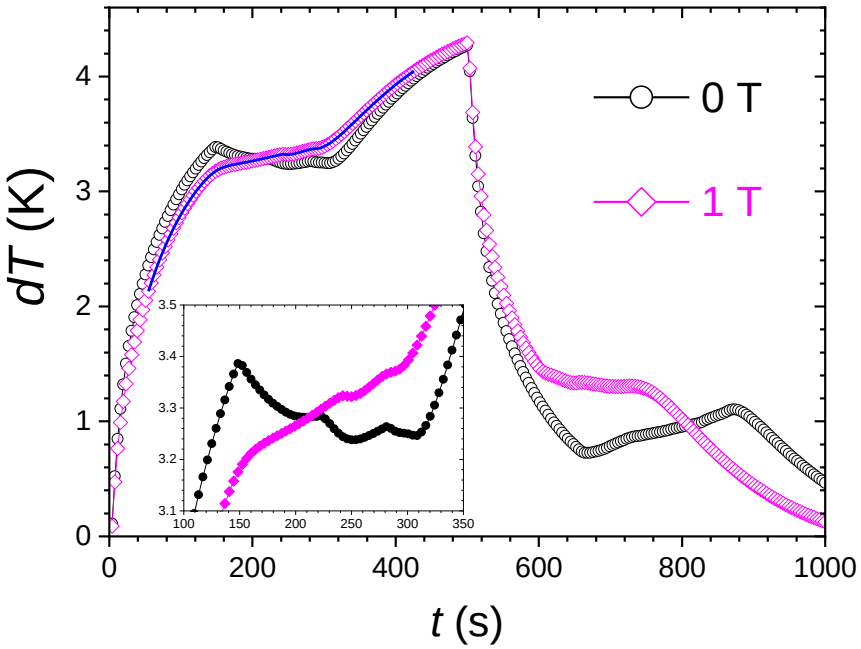

FIG. 5. Temporal profiles of the thermal response resulting from a heat pulse applied either in zero field or in 1 T. The parameters of the heat pulse are the same in both cases (P_{heat} =780 µW for ΔT_{pulse} = 4 K). Owing to the field dependence of T_{tr}, the base temperature (T_b) is 205 K in zero-field and 209 K in 1 T. To allow better comparison of the two measurements, one plotted $dT(t)=T(t)-T_b$. The blue line for 1 T materializes the part of the branch used to derive $C_s(T)$ in Fig. 6(a). The inset is an enlargement of the transitional regime upon warming.

Then, these heat capacity data allows one to calculate the temperature dependence of the total entropy $S(T) = S^* + \int_{T^*}^{T} \left[\frac{C_S(T)}{T}\right] dT$, where T^* is the lowest boundary of the T range in Fig. 6(a) and $S^* = S(T^*)$. The result is shown in Fig. 6(b), along with linear extrapolations from below and above the transition, as well as a vertical line crossing the curve at T_{tr}. This plot clearly exhibits a step in $S(T)$ as expected for a FOT; the estimate of its height (i.e., the

ΔS_{tr} value) is somewhat a matter of criteria. At first glance, one would be tempted to define ΔS_{tr} by the spacing between the two circles on the construction of Fig. 6(b) (leading to ~ 11.5 $JK^{-1}kg^{-1}$). However, to be consistent with the boundaries of the transition defined by the location of the plateau-like regime, one should rather consider the squares marked on Fig. 6(b). Doing so, the associated ΔS_{tr} is found to be 9.3 $JK^{-1}kg^{-1}$, leading to $L \sim 2.0$ Jg^{-1}. Re-starting from the raw data, we also performed an analysis in terms of $P_L(t)$ via Eq. (4) whose results is displayed on Fig 6(c) (for warming). It turns out that the integration yields 2.1 J g^{-1}, which is well consistent with the above L value. It can also be compared to the value derived from the CC analysis. According to Fig. 4(b), one expects ΔS_{tr} (1T) ~ 8.5 $JK^{-1}kg^{-1}$ corresponding to L(1T) ~ 1.8 Jg^{-1}, a value which is also in reasonable agreement with that derived from the $P_L(t)$ analysis.

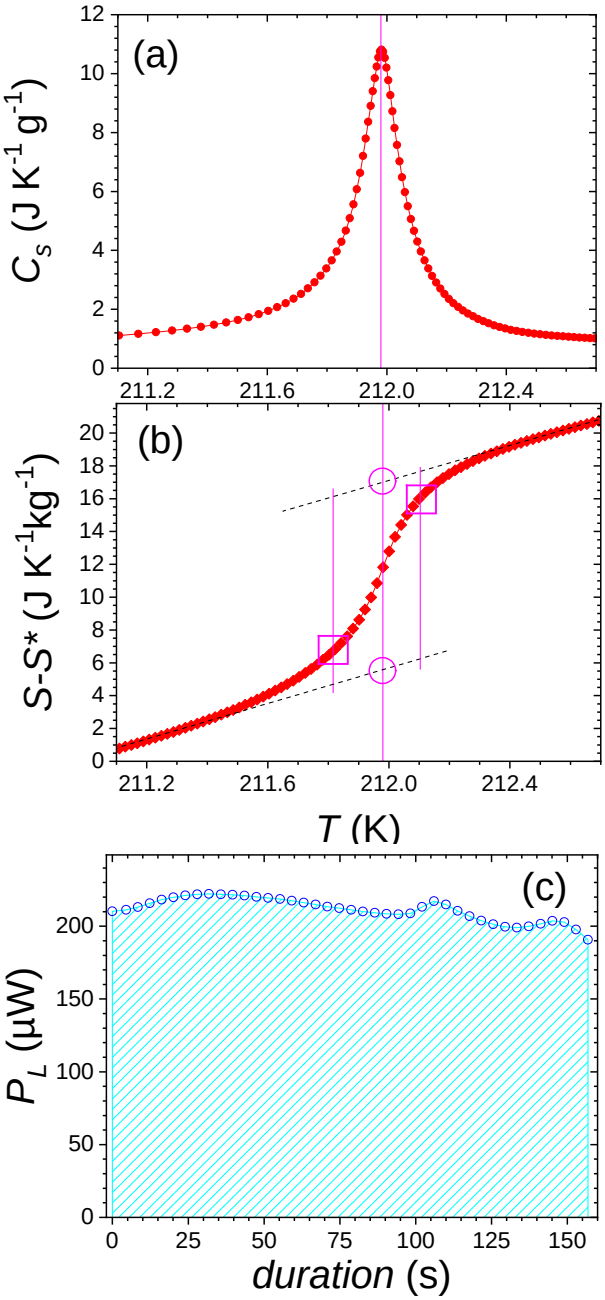

FIG. 6. Analysis of the relaxation data in 1 T along the heating branch. Panel (a) is a standard analysis in terms of heat capacity, obtained from the profile of Fig. 5 by using Eq. (5). Panel (b) is derived from (a) by integrating C_s/T starting from a reference temperature T^* = 210.95 K. Panel (c) corresponds to the analysis via Eq. (4).

IV. DISCUSSION

Using semi-adiabatic relaxation calorimetry, we have suggested a mode of analysis able to account for exotic phenomena encountered in FOT's, such as the recalescence/antirecalescence effects and the presence of spikes in the latent heat exchange. Several results come to support the reliability of this approach. First, it is found that the peculiar behaviors derived from this approach (reversed trends in the thermal response and

burstlike heat exchange per unit time) are confirmed by DSC experiments; since DSC is known to be the reference technique to deal with the heat exchanges at FOT's, this consistency provides valuable support to the analysis in terms of power of latent heat $P_L(t)$. From a more quantitative viewpoint, several issues also deserve to be emphasized: (i) the overall latent heat L derived from integration of $P_L(t)$ turns out to be independent of the recording parameters; (ii) this L value is in agreement with that derived from the CC equation applied to magnetic data; (iii) this L value is also consistent with that derived from the $C_s(T)$ curve obtained by a standard analysis (possible in 1 T).

On the other hand, this approach has several limitations. First, it relies on the theoretical expectation of a null dT_s/dt at the FOT; any deviation from this assumption will introduce an experimental uncertainty in our results; to quantify it, let us consider an estimate of the lattice heat capacity at the FOT derived from extrapolations of the heat capacity data from each side of the transition (C_{lat} ~ 425 µJ K^{-1} mg^{-1}) and a mean $\langle dT_s/dt \rangle$ approximated by the average dT_p/dt over the plateau-like transformation (e.g., -0.0028 K/s in Fig. 1); doing so, one obtains $C_{lat}\langle dT_p/dt \rangle \approx 18$ µW, a value which remains much smaller than the P_L values obtained by the analysis (~500 µW). Second, it must be stressed that the definition of the boundaries of the time window over which $P_L(t)$ is calculated is subject to a notable uncertainty. For instance, moving this interval by one data spacing on both side of $P_L(t)$ in Fig. 6(c) would yield an uncertainty of ~ 5% on the L value. Third, the profile of $P_L(t)$ suffers from a poor resolution in time, which is given by the data spacing of ~ 4 s (a limitation imposed by the recording system). This prevents from the observation of any dynamics faster than this time scale. Furthermore, there is another source of limitation which is still more detrimental. Indeed, contrary to the DSC experiments where one measures directly the heat exchanges, in our case this quantity is only indirectly reflected by the temperature of the platform. Assuming that the latent exchange can be inhomogeneous, one must first consider the time constant associated to the thermalisation of the sample itself; this is typically given by the relationship $\tau_s = (e^2/4)/\alpha$, where e is the sample thickness and α the diffusivity. With e = 0.4 mm and α ~ 2 mm^2/s, it turns out that it yields a very short time of ~ 0.02 s which is thus negligible. Actually, the limiting time constant in our case is that related to the thermal contact sample/platform, which can be approximated by $\tau_g = R_g C_{lat}$, where R_g is the thermal resistance of the grease ($= 1/K_g$) and C_{lat} the phononic heat capacity at the FOT (~ 425 µJ K^{-1} mg^{-1}). The former parameter can be evaluated from the two time constants (τ_1 and τ_2) obtained from the standard fitting of the relaxation profiles out of the transitional regime (see

supplementary material) while the latter depends on the mass (~ 15.8 mg) of the sample. In our experiment, one obtains $K_g \sim 735$ µW/K and $C_{lat} \sim 6715$ µJ/K, leading to $\tau_g \sim 9$ s. As a consequence, our system cannot account for well separated spikes on the heat flow, and can just exhibit slight modulations of the $P_L(t)$ profile.

Recalescence is a well documented phenomenon, whereas antirecalescence is much less common, even though we note that a signature similar to ours has been reported in metallic Dy (dT ~ - 0.4 K) [22]. Focusing on the magnetocaloric materials, reversed trends of similar amplitudes (~ 0.1 K) have been observed in compounds of the La-(Fe,Mn,Si) system [11], while much larger effects can take place in the $(Mn,Fe)_2(P,Si)$ materials, but only along the first cooling (see the supplementary material). It is important to emphasize that the size of these temperatures increments depends on the value of the thermal linkage to the bath. In our semi-adiabatic set-up, this thermal resistance (towards the bath) is substantially larger (i.e., $1/K_w$ ~ 6000 K/W) than the values of the order of 500 K/W reported in DSC experiments [10,25].

Considering the case of magnetic FOT's, the first observations of "spiky patterns" were reported in ultra-pure Er and in $(Hf,Ta)Fe_2$ intermetallics [4-5] Note that these studies involved different calorimetric set-ups and different types of magnetic transitions. In each case, two or three bursts take place along the transformation. More recently, several studies reporting the same type of features were carried out in magnetocaloric materials. For instance, DSC investigations revealed six spikes along the transition of a LaFeSiCo material, [10] while a hydrogenated LaFeSiMn compound exhibited two wider peaks but with a clear sub-structure [11]. Actually, the comparisons between experiments must be regarded cautiously since the results strongly depend on the specific resolution of each device. Besides, other studies prefer to show the DSC data in terms of a generalized vision of the specific heat including the latent heat. In the first reports, this has yielded high peaks in $C_s(T)$ exhibiting a spiky substructure [26-27]. More recent studies reported signatures of the transition in $C_s(T)$ taking the form of well separated peaks [28].

Let us now briefly comment on the possible origin of this peculiar phenomenon. In the case of Er, the authors suggested that the bursts may reflect the existence of metastable states separating the start and end phases of the FOT, [4] whereas in the case of $(Hf,Ta)Fe_2$ these bursts were rather ascribed to nucleation and growth events in different regions of the samples [5]. Besides, in substituted materials like LaFeSiCo, other authors suggested the possibility of a relationship between the bursts and a distribution of local values of T_c. Another viewpoint

is to consider that even in case of a single T_c and without intermediate phases, one can expect such a burstlike response owing to the mismatch of the crystalline structure between the two phases separated by the FOT [29]. We note that all materials in which burstlike transitions are present exhibit substantial changes in structural parameters at the transition. In the case of our LaFeSiCo, the transition is isomorphic and one can estimate from the literature $\Delta V/V \sim 1\%$ (from PM to FM) [19-20]. Such mismatch necessarily generates strains at the interfaces PM/FM and long range stresses, which yield the rise of an elastic energy opposing the development of the transition. This underlying energy can even delay the start of the transformation expected when crossing T_c either upon cooling or warming, leading to undercooling and overheating effects. When the transition starts, it exhibits a very abrupt character: the larger the overshooting, the steeper the triggering. For materials which are characterized by a particularly large latent heat (such as the most performing magnetocaloric materials) the resulting heat flows can be very large. This process is most likely at the origin of the recalescence and antirecalescence phenomena.

Then, the development of the transition is associated to the diffusion of the front between the two phases (PM/FM in our case). We support the idea that the jerky character of the transformation corresponds to transient pinning/depinning events along this front [11,25,30]. The most obvious cause for transient blockings is the rise in elastic energy, but one should also consider a thermal effect, since the latent heat exchanges associated with the move of the front tend to oppose it [25]. Considering for instance the PM to FM transition (i.e. upon cooling), the transformation is exothermic, favoring a local increase in temperature which thereby yields an inhibiting effect. Whatever the pinning mechanisms at play, the depinning path followed within the sample will depend on the details of the microstructure (such as secondary phases, defects and grain boundaries). Therefore, even though the basic origin of the "spiky patterns" is intrinsic (structural mismatch), the sample response necessary involves features of its microstructure, which are extrinsic. Both aspects are thus intimately entangled in the description of the burstlike transitions.

V. CONCLUSION

We have proposed an analysis of semi-adiabatic relaxation data allowing to investigate two phenomena sometimes encountered in FOT': reversed trends in the thermal response (recalescence/antirecalescence) and presence of spikes in the time dependent exchange of latent heat at the transition (so-called "spiky pattern" or "peak forest" [28] effects). Both

phenomena can emerge in materials exhibiting a structural mismatch between the two phases at each side of the transition, as well as a large value of latent heat. They have known a recent surge of interest in the context of the studies on intermetallics showing a giant magnetocaloric effect that are targeted for applications in magnetic refrigeration. The presently investigated $LaFe_{10.77}Si_{1.23}Co_{0.28}$ compound belong to this class of materials. It must be acknowledged that the reported approach is less direct and powerful than DSC devices to detect the fine time structure of heat flows at a FOT. However, our approach allows such basic phenomena to be investigated in widely used commercial devices, and it also allows a direct connection with the specific heat measurements on each side of the transition (which can be performed accurately with the same sample mounting).

Regarding the "reversed trends", the most puzzling effect is that found on the heating branch (antirecalescence) which may appear at first glance less intuitive than its recalescence counterpart. Yet, it just demonstrates that the sample is active when crossing T_{tr} upon warming, merely as it is along the reverse path; upon warming, the transition is endothermic and once the transition has been triggered, the sample pumps heat to the platform to ensure the development of the transformation with its own time constant (instead of simply waiting for the heater located on the platform to provide this latent heat). Note that these effects of recalescence/antirecalescence cannot be regarded as basic features of the material since their observation depends on extrinsic factors, such as the strength of the thermal coupling sample/environment.

What is more tricky in the present data is the "spiky pattern". Even though there is still debate about the origin of this effect, it is quite clear that it reflects a process of the transformation that is irregular in time and inhomogeneous in space. We favor an interpretation in terms of friction related to the mismatch between the two phases in competition at the transition. Increase in elastic energy can locally exceed the energetic gain associated with a smooth development of the transition. Depinning takes place when the driving force allows to overcome the barriers associated to the strains. Such a sequential process is thought to be at the origin of the jerky displacement of the transition front (FM-PM).

It is obvious that much could be learned from local techniques like magneto-optics, as already investigated in the case of LaFeSiCo materials (e.g., [10]). To go still further, it might be interesting to explore complementary techniques with enhanced resolutions, both in space and time, such as Magnetic Force Microscopy as recently used in FeRh materials [31-32].

Extending this type of local probes to investigate the spatio-temporal features at the burstlike transitions in FOT's is a very appealing challenge that would deserve to be taken up.

SUPPLEMENTARY MATERIAL

See the supplementary material for estimates of the shift between T_p and T_s within the transitional regime, and of the entropy step at the transition from the Clausius-Clapeyron equation.

ACKNOWLEDGMENTS

This work is part of the CoolMagEvo ANR-17-CE05-0036 project, from the Research Programme "Energy, clean, safe and efficient (DS02) 2017" of the french National Research Agency (ANR). The work at Inner Mongolia Normal University is supported by the National Natural Science Foundation of China (grant n° 51961033).

AUTHOR DECLARATIONS

The authors have no conflicts to disclose.

APPENDIX

The conductive leak term

The large temperature increment used in our pulses can generate a substantial gradient of temperature along the wires ensuring the thermal leaks towards the 'bath" (this role of "bath" is played in our system by the puck, a bulk metallic piece onto which the wires are soldered). Since the thermal conductivity of the wires (Au-Pd alloy) is temperature dependent, this gradient must be taken into account to accurately quantify the term P_{cond}. The situation one has to face is schematically shown in Fig. 7.

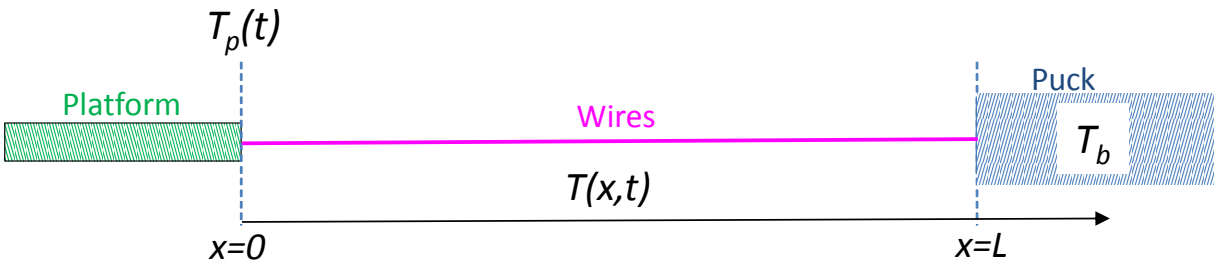

FIG. 7. Schematic picture of the thermal link platform/bath via the wires (there are eight wires but only one is shown here). At the boundary platform/wire the temperature is $T_p(t)$, while it should keep constant and equal to T_b at the boundary wire/puck.

In case of a small ΔT_{pulse}, one can reasonably assume an homogeneous conduction involving a simple K_w term. The conductance K_w is related to the conductivity k_w via the relationship $K_w = 8k_w(s/L)$, where L and s are the length and cross section of each wire, respectively. In the standard analysis, one can consider

$P_{cond} = -K_w(T_p - T_b)$, with $K_w \sim K_w(T_b)$.

For an inhomogeneous conduction (change of local k_w along the wire) this equation must be replaced by

$P_{cond} = -K_{eff}(T_p - T_b)$, with $\frac{1}{K_{eff}} = \int_0^L \frac{dx}{8s\, k_w(x)}$.

The x-dependence of k_w is actually a function of the temperature T. Over the limited range of temperature used along the pulse, one can consider a linear dependence $k_w(T) = a + bT$.

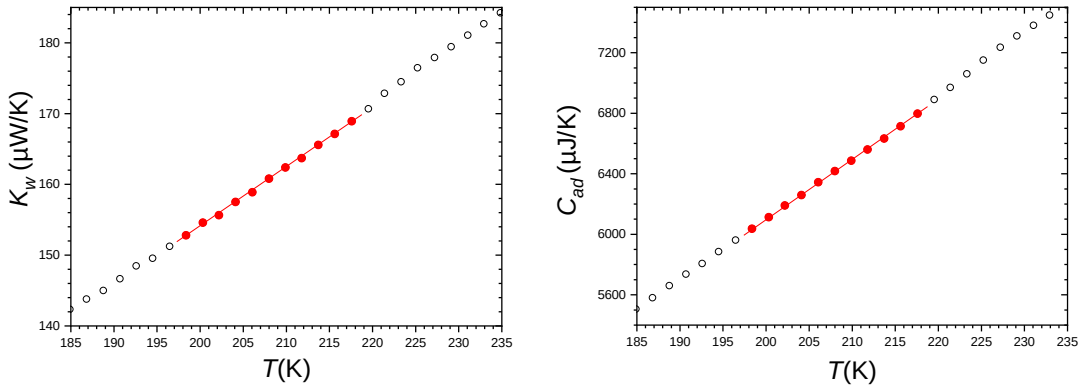

FIG. 8. Experimental determinations of $K_w(T)$ and $C_{ad}(T)$ derived from the background measurements. The red data points show the range of the pulses, over which linear fittings can be applied.

Experimentally, one gets access to the conductance K_w in the background measurements of the set (platform+grease): $K_w(T) = 8k_w(T)(s/L) = 8(a + bT)(s/L) = A + BT$ (see Fig. 8). Assuming a linear profile of T along the wire (a reasonable approximation, even though the exact solution is more complex), one can consider $T(x) \approx T_p - (T_p - T_b)/(x/L)$. This leads to $\frac{1}{K_{eff}} \approx \frac{1}{8s}\int_0^L \frac{dx}{a+b[T_p-(T_p-T_b)/(x/L)]}$, and one finally arrives at the expression

$$P_{cond} \approx -\left\{\frac{B(T_p-T_b)}{ln\left(\frac{A+BT_p}{A+BT_b}\right)}\right\}(T_p - T_b)\,. \qquad \text{(A1)}$$

This relationship is quite different from that of the homogeneous case, i.e. $P_{cond} \approx -(A + BT_b)(T_p - T_b)$.

The radiative leak term

Still owing to the size of the temperature increment, the difference between T_s and T_b can become large enough to generate a non-negligible radiative term at high temperature. The radiative term between the external sample surface S (at the temperature T_s) and the metallic surface of the protective cap (at the temperature T_b) is given by the expression $P_{rad} = -\sigma_T\, S\, \varepsilon_s(T_s^4 - T_b^4)$, where σ_T is the Stefan-Boltzmann constant (5.67 10^{-8} W m^{-2} K^{-4}), S the radiative surface of the sample and ε_s its infrared emissivity. Considering that the temperature difference remains moderate, i.e. $(T_s - T_b)/T_b << 1$, one can use the relationship

$$P_{rad} \approx -4\,\sigma_T\, S\, \varepsilon_s(T_s - T_b)T_b^3 \qquad \text{(A2)}$$

DATA AVAILABILITY

The data that supports the findings of this study are available within the article and its supplementary material.

REFERENCES

[1] W. F. Barrett, Nature 60, 173 (1899).

[2] E. Reed-Hill, "Physical Metallurgy Principles", VanNostrand, Princeton, NJ (1964).

[3] J. Hopkinson, Proc. R. Soc. Lond. 45, 455 (1889).

[4] K. A. Gschneidner, V. K. Pecharsky, and D. Fort, Phys. Rev. Lett. 78, 4281 (1997).

[5] P. Bag, R. Rawat, P. Chaddah, P. D. Babu, and V. Siruguri, Phys. Rev. B 93, 014416 (2016).

[6] T. Plackowski, Y. Wang, A. Junod, Rev. Sci. Instrum. 73, 2755 (2002).

[7] J. Marcos, F. Casanova, X. Batlle, A. Labarta, A. Planes, L. Mañosa, Rev. Sci. Instrum. 74, 4768 (2003).

[8] V. Basso, M. Kuepferling, C. P. Sasso, L. Giudici, Rev. Sci. Instrum. 79, 063907 (2008).

[9] S. Jeppesen, S. Linderoth, N. Pryds, L. Theil Kuhn, J. Buch Jensen, Rev. Sci. Instrum. 79, 083901 (2008).

[10] M. Kuepferling, C. Bennati, F. Laviano, G. Ghigo, V. Basso, J. Appl. Phys. 115, 17A925 (2014).

[11] C. Bennati, L. Gozzelino, E. S. Olivetti, V. Basso, Appl. Phys. Lett. 109, 231904 (2016).

[12] R. Bachmann, F. J. DiSalvo, T. H. Geballe, R. L. Greene, R. E. Howard, C. N. King, H. C. Kirsch, K. N. Lee, R. E. Schwall, H.-U. Thomas, R. B. Zubeck, Rev. Sci. Instrum. 43, 205 (1972).

[13] PPMS Heat Capacity Option User's Manual, 1085-150, Rev. M6 (February 2015), Quantum Design, San Diego.

[14] J. S. Hwang, K. J. Lin and C. Tien, Rev. Sci. Instrum. 68, 94 (1997).

[15] J. C. Lashley, M. F. Hundley, A. Migliori, J. L. Sarrao, P. G. Pagliuso, T.W. Darling, M. Jaime, J. C. Cooley,W. L. Hults, L. Morales, D. J. Thoma, J. L. Smith, J. Boerio-Goates, B. F. Woodfield, G. R. Stewart, R. A. Fisher, N. E. Phillips, Cryogenics 43, 369 (2003).

[16] V. Hardy, Y. Bréard and C. Martin, J. Phys. Cond. Matter 21, 075403 (2009).

[17] H. Suzuki, A. Inaba, and C. Meingast, Cryogenics 50, 693 (2010).

[18] F. Guillou, P. Courtois, L. Porcar, D. Bourgault, V. Hardy, J. Phys. D:Appl. Phys. 45, 255001 (2012)

[19] A. Fujita, S. Fujieda, K. Fukamichi, H. Mitamura, T. Goto, Phys. Rev. B 65, 014410 (2001).

[20] F. X. Hu, J. Gao, X. L. Qian, M. Ilyn, A. M. Tishin, J. R. Sun, B. G. Shen, J. Appl. Phys. 97, 10M303 (2005).

[21] PPMS Application Note, 1085-159 (April 2014), Quantum Design, San Diego.

[22] V. K. Pecharsky, K. A. Gschneidner, Jr., D. Fort, Scr. Mater. 35, 843 (1996).

[23] To deal with FOT's in our device, the user can utilize the "single-curve slope analysis", which generates a point-by-point analysis of each branch of the relaxation response [13]. This built-in tool allows to adjust the width of the time window over which the dT_p/dt is calculated.

Although, it can be useful to smooth noisy data, improper use of this option can yield completely artificial results, especially in presence of a "reversed trend" by producing a misleading *C(T)* peak (e.g., if the averaging range is wider than the duration of the transition).

[24] F. Guillou, H. Yibole, Z. Q. Ou, E. Brück, O. Tegus, Scripta Materialia 160, 81 (2019).

[25] M. Piazzi, C. Bennati, V. Basso, Phys. Rev. Applied 8, 044023 (2017).

[26] M. Kuepferling, C. P. Sasso, V. Basso, EPJ Web Conf. 40, 06010 (2013).

[27] V. Basso, M. Kuepferling, C. Curcio, C. Bennati, A. Barzca, M. Katter, M. Bratko, E. Lovell, J. Turcaud, L. F. Cohen, J. Appl. Phys. 118, 053907 (2015).

[28] F. Erbesdobler, C.R.H. Bahl, R. Bjørk, and K.K. Nielsen, J. Appl. Phys. 127, 095102 (2020).

[29] H. N. Bez, K. K. Nielsen, A. Smith, P. Norby, K. Ståhl, and C. R. H. Bahl, Appl. Phys. Lett. 109, 051902 (2016).

[30] E. Lovell, M. Bratko, A. D. Caplin, and L. F. Cohen, J. Phys. D: Appl. Phys. 50, 424004 (2017).

[31] M. Manekar, S. B. Roy, J. Phys. D: Appl. Phys. 41, 192004 (2008).

[32] J. L. Warren, C. W. Barton, C. Bull, T. Thomson, Sci. Rep. 10, 4030 (2020).